Analysis of two-body charmed B meson decays in factorization-assisted topological-amplitude approach

Si-Hong Zhou,[1] Yan-Bing Wei,[1] Qin Qin,[1] Ying Li,[2,4] Fu-Sheng Yu,[3] and Cai-Dian Lü[1,4]

[1]*Institute of High Energy Physics, Beijing 100049, People's Republic of China*
[2]*Department of Physics, Yantai University, Yantai 264005, People's Republic of China*
[3]*School of Nuclear Science and Technology, Lanzhou University, Lanzhou 730000, People's Republic of China*
[4]*State Key Laboratory of Theoretical Physics, Institute of Theoretical Physics, Chinese Academy of Sciences, Beijing 100190, People's Republic of China*

(Received 17 September 2015; published 9 November 2015)

Within the factorization-assisted topological-amplitude approach, we study the two-body charmed B meson decays $B_{u,d,s} \to D^{(*)}M$, with M denoting a light pseudoscalar (or vector) meson. The meson decay constants and transition form factors are factorized out from the hadronic matrix element of topological diagrams. Therefore, the effect of SU(3) symmetry breaking is retained, which is different from the conventional topological diagram approach. The number of free nonperturbative parameters to be fitted from experimental data is also much less. Only four universal nonperturbative parameters χ^C, ϕ^C, χ^E and ϕ^E are introduced to describe the contribution of the color-suppressed tree and W-exchanged diagrams for all the decay channels. With the fitted parameters from 31 decay modes induced by $b \to c$ transition, we then predict the branching fractions of 120 decay modes induced by both $b \to c$ and $b \to u$ transitions. Our results are well consistent with the measured data or to be tested in the LHCb and Belle-II experiments in the future. Besides, the SU(3) symmetry breaking, isospin violation and CP asymmetry are also investigated.

DOI: 10.1103/PhysRevD.92.094016 PACS numbers: 13.25.Hw

I. INTRODUCTION

Due to the large mass and fast weak decay property of the top quark, B mesons are the only weakly decaying mesons containing quarks of the third generation. Their nonleptonic weak decays provide direct access to the parameters of the Cabibbo–Kobayashi–Maskawa (CKM) matrix and to the study of CP violation (for reviews, see, for examples, Refs. [1,2]). Simultaneously, the studies of these decays can also provide some insight into the long-distance nonperturbative structure of QCD as well as some hints of the new physics beyond the standard model (SM). To achieve these goals, the *BABAR* and Belle experiments at the e^+e^- B-factories [3] and the LHCb experiment [4] at the LHC have already performed high precision measurements of nonleptonic weak decays. In the era of the Belle-II [5] and LHCb upgrade [4], the experimental analysis will be pushed toward new frontiers of precision.

In particular, the direct CP violation in a decay process requires at least two contributing amplitudes with different weak and strong phases. In the SM, the weak phases can be accommodated in the CKM matrix, while no satisfactory first-principle calculations have yielded the strong phases till now. To study the information of strong phases from the nonleptonic B decays is tough work. The basic theoretical framework for the nonleptonic B decays is based on the operator product expansion and renormalization group equation, which allow us to write the amplitude of a decay $\bar{B} \to f$ generally as follows:

$$\mathcal{A}(\bar{B} \to f) = \langle f|\mathcal{H}_{\rm eff}|\bar{B}\rangle = \frac{G_F}{\sqrt{2}} V_{\rm CKM} \sum_i C_i(\mu)\langle f|O_i(\mu)|\bar{B}\rangle, \quad (1)$$

where $\mathcal{H}_{\rm eff}$ is the effective weak Hamiltonian, with $O_i(\mu)$ denoting the relevant local four-quark operators, which govern the decays in question. The CKM factors $V_{\rm CKM}$ and the Wilson coefficients C_i describe the strength with which a given operator enters the Hamiltonian. Now, the only challenge for theorists is how to calculate the matrix elements $\langle f|O_i(\mu)|\bar{B}\rangle$ in QCD reliably. For decades we have applied the "factorization" hypothesis to estimate the matrix element of the four-quark operators through the product of the matrix elements of the corresponding quark currents. In the 1980s, the "color transparency" viewpoints [6–8] were used to justify this concept, while it could be put on a rigorous theoretical basis in the heavy-quark limit for a variety of B decays about ten years ago [9–11]. Alternatively, another useful approach is provided by the decomposition of their amplitudes in terms of different decay topologies and to apply the SU(3) flavor symmetry of strong interactions to derive relations between them [12]. Supplemented by isospin symmetry, the approximate SU(3) flavor symmetry and various "plausible" dynamical assumptions, the diagrammatic approach has been used extensively for nonleptonic B decays [13].

Among B decays, the charmed hadronic B mesons decays $B \to D^{(*)}M$, where M is a light meson, are of great

interest for several reasons. First, due to the existence of the charm quark, the charmed hadronic decay processes have no contribution from penguin operators, so theoretical uncertainties involved in the relevant QCD dynamics become much less. Second, for the $b \to c$ transiting processes, since the CKM factors are real, the phases associated with these decay amplitudes afford us the information of clean strong interactions. Third, for some typical decays such as $\bar{B}_s^0 \to D_s^{(*)\pm} K^{\mp}$ and $\bar{B}_d^0 \to D^{(*)\pm}\pi^{\mp}$, both $b \to c$ and $b \to u$ transitions contribute to their amplitudes, the interferences between which will allow us to extract the CKM phase γ effectively [14]. Lastly, these processes serve as a good testing ground for various theoretical issues in hadronic B decays, such as factorization hypothesis, SU(3) symmetry breaking, and isospin violation. Experimentally, plenty of two-body charmed hadronic B decays have been observed from the heavy flavor experiments, such as Belle, *BABAR*, D0, CDF, and LHCb [15]. Besides the available data, many new modes are being measured in the LHCb. In the theoretical side, much attention has already been paid to these charmed hadronic B decays. The color-favored decays $B \to D^{(*)}\pi$ were first explored in the framework of the factorization hypothesis [7,8]. Including the next-leading-order corrections of vertexes, the factorization of this kind of processes has been proven within the QCD factorization approach [9] and the soft-collinear effective theory [11], which implies the final-state interactions of these decays are small. However, the color-suppressed modes $B^0 \to \bar{D}^0\pi^0$ were found with a very large branching ratio experimentally, which provides evidence for a failure of the naive factorization and for sizeable relative strong-interaction phases between different isospin amplitudes [16]. This was confirmed in the perturbative QCD (PQCD) approach based on k_T factorization [17–19], where the end point singularity was killed by keeping the transverse momentum of partons. The rescattering effects of $B \to D^{(*)}M$ had also been studied within some models [20]. Under the assumption of the flavor SU(3) symmetry, the global fits were performed in the topological quark diagram approach [21], where the magnitudes and the strong phases of the topologically distinct amplitudes were studied, but the information of SU(3) asymmetry was lost. Due to the large difference between the pseudoscalar and vector meson, their χ^2 fit has to be performed for each category of decays to result in three sets of parameters.

Recently, in order to study the two-body hadronic decays of D mesons, the factorization-assisted topological-amplitude (FAT) approach was proposed [22,23], which combines the conventional factorization approach and topological-amplitude parametrization. We will introduce the framework in the next section in detail. By involving the nonfactorizable contributions and the SU(3) symmetry breaking effect, most theoretical predictions of the D decays are in better agreement with experimental data, and the long-standing puzzle from the $D^0 \to \pi^+\pi^-$ and $D^0 \to K^+K^-$ branching fractions can be well solved [22]. In this work, we shall generalize the FAT approach to study the two-body charmed nonleptonic B mesons decays. With the available experimental data for 31 decay channels, we shall fit the only four theoretical parameters, reducing from the 15 parameters introduced in Ref. [21]. The SU(3) asymmetries and their implications will also be discussed. The predicted results for all the 120 decay channels can be tested in the running LHCb experiment, future Belle-II experiment, and even high energy colliders in the future.

This manuscript is organized as follows. In Sec. II, we introduce the framework of the FAT approach and fit the four universal parameters from the available data induced by $b \to c$ transition. In Sec. III, we predict the branching fractions of decays induced by $b \to u$ transition with the assumption that the numerical values of four universal parameters are the same as those of decays of $b \to c$ transition. The discussions on the phenomenological implications will be given in Sec. IV. At last, we shall summarize this work in Sec. V.

II. CKM-FAVORED DECAYS INDUCED BY $b \to c$ TRANSITION

A. Framework of FAT approach

When discussing the charmed B decays, a new intermediate scale (m_c) is introduced, which satisfies the mass hierarchy $m_b > m_c > \Lambda_{\rm QCD}$. The perturbative theory may not be valid in the scale (m_c), implying the failure of QCD factorization. Thus, the best way is to extract the information of them from experimental data. In the conventional topological diagrammatic approach, the amplitude of each diagram was proposed to be extracted directly [21] from experimental data. To achieve this goal, the flavor SU(3) symmetry has to be employed, which works well in the two-body charmless B decays [13] due to the negligible mass of the light meson. However, in dealing with the D meson decays [24], it is found that only the experimental data of Cabibbo-favored decay modes can be used, which implies that the SU(3) breaking effects are sizable in the D decays. As for the charmed B decays, the effects from SU(3) asymmetry are also expected to be sizable that may not be negligible. Even if people ignore the SU(3) breaking effect of the $\pi - K$ difference, the $\chi 2$ fit can only be done separately in three categories of decays, namely, $B \to DP$, $B \to DV$, and $B \to D^*P$, with five free parameters in each group [21]. Obviously, the predictive power is lost with 15 parameters to be fitted from experimental data. With some SU(3) breaking effects input by hand, the number of free parameters becomes 21 in the χ^2 fit of Ref. [21], which is surely not satisfactory.

The FAT approach was first proposed for studying the two-body hadronic D mesons decays [22,23], which is a

great success in the extraction of strong phases for the CP asymmetry study. There are five steps in the FAT approach. First, similar to the topological diagrammatic approach [21], the two-body hadronic weak decay amplitudes are decomposed in terms of some distinct quark diagrams, according to the weak interactions and flavor flows with all strong-interaction effects encoded. In this way, the non-negligible nonfactorizable contributions are involved, and hence the results would be more accurate if their values can be extracted from experimental data. In the case of charmed hadronic decays of B mesons, four kinds of relevant quark diagrams are involved, namely, the color-favored tree diagram T, the color-suppressed tree diagram C, the W-exchange annihilation-type diagram E, and the W-annihilation diagram A. Second, in order to keep the SU(3) breaking effects in the decay amplitudes, we factorize the decay constants and form factors formally from each topological amplitude. The topological amplitude is then only universal for all decay channels after factorization of those hadronic parameters. Third, the QCD factorization, the perturbative QCD based on k_T factorization, together with the soft-collinear effective theory have all proven factorization for the color-favored topology diagram [9,11,17]. The T amplitude is then safely expressed by the products of the transition form factor, decay constant of the emitted meson, and the short-distance dynamics Wilson coefficients, where the latter are related to the four-fermion operators. No free parameter will be introduced in the T diagram calculations. Fourth, for the remaining color-suppressed diagram and W-exchange diagram (W), we also factorize them into the decay constants and form factors with only four universal free parameters χ^C, ϕ^C, χ^E and ϕ^E the explicit values of which will be fitted from the abundant experimental data simultaneously. Lastly, with the four fitted universal nonperturbative parameters, we then make predictions for all the hadronic charmed B decays $B_{u,d,s} \to D^{(*)}P(V)$ and $B_{u,d,s} \to \bar{D}^{(*)}P(V)$, where P and V denote pseudoscalar and vector mesons, respectively.

According to the effective Hamiltonian [25], these decays can be classified into two groups: the CKM-favored processes induced by $b \to c$ transition and the CKM-suppressed ones induced by $b \to u$ transition. We first discuss the relevant effective weak Hamiltonian for the CKM-favored transition $b \to cq\bar{u}$ $(q = d, s)$, which is given by [25]

$$\mathcal{H}_{\rm eff} = \frac{G_F}{\sqrt{2}} V_{cb}V_{uq}^*[C_1(\mu)O_1(\mu) + C_2(\mu)O_2(\mu)] + \text{H.c.}, \tag{2}$$

where G_F is the Fermi coupling constant, V_{cb} and V_{uq} are the relevant CKM matrix elements, and $C_{1,2}$ are the Wilson coefficients. The tree-level current-current operators are

$$\begin{aligned} O_1 &= \bar{q}_\alpha \gamma^\mu (1-\gamma_5) u_\beta \bar{c}_\beta \gamma_\mu (1-\gamma_5) b_\alpha, \\ O_2 &= \bar{q}_\alpha \gamma^\mu (1-\gamma_5) u_\alpha \bar{c}_\beta \gamma_\mu (1-\gamma_5) b_\beta, \end{aligned} \tag{3}$$

where α and β are the color indices. The topological diagrams in the $b \to c$ transitions include color-favored tree emission diagram T, color-suppressed tree emission C, and W-exchange diagram E, as shown in Fig. 1. Note that the W-annihilation diagram does not occur in the $b \to c$ transition processes, and the E diagram occurs only in the $\bar{B}_d^0$ and $\bar{B}_s^0$ decays. It is apparent that the T diagram emits a light meson and recoils a charmed meson, while for the C diagram, the charmed meson is emitted, and the light meson is recoiled.

In terms of the factorization hypothesis, the three diagrams of the $\bar{B} \to DP$ modes can be written as

$$T_c^{DP} = i\frac{G_F}{\sqrt{2}} V_{cb}V_{uq}^* a_1(\mu) f_P (m_B^2 - m_D^2) F_0^{B\to D}(m_P^2), \tag{4}$$

$$C_c^{DP} = i\frac{G_F}{\sqrt{2}} V_{cb}V_{uq}^* f_D (m_B^2 - m_P^2) F_0^{B\to P}(m_D^2) \chi_c^C e^{i\phi_c^C}, \tag{5}$$

$$E_c^{DP} = i\frac{G_F}{\sqrt{2}} V_{cb}V_{uq}^* m_B^2 f_B \frac{f_{D_{(s)}} f_P}{f_D f_\pi} \chi_c^E e^{i\phi_c^E}, \tag{6}$$

where the subscript c stands for the processes induced by $b \to c$ transition and f_P and f_D stand for the decay constants of the pseudoscalar meson and D meson, respectively. $F_0^{B\to D}$ and $F_0^{B\to P}$ are the scalar form factors of the $\bar{B} \to D$ and $\bar{B} \to P$ transitions. Here we have followed the conventional Bauer–Stech–Wirbel definition for form factors $F_{0,1}^{BP}$ and A_0^{BV} [7]. The inner effective Wilson coefficient is

$$a_1(\mu) = C_2(\mu) + \frac{C_1(\mu)}{3}. \tag{7}$$

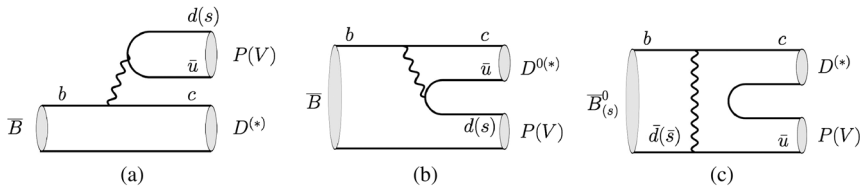

FIG. 1. Topological diagrams in the $b \to c$ transitions: (a) the color-favored tree diagram, T; (b) the color-suppressed tree diagram, C; and (c) the W-exchange annihilation-type diagram, E. Note that the E diagram occurs only in the $\bar{B}_d^0$ and $\bar{B}_s^0$ decays.

For the T diagram, the nonfactorizable contribution is so small that can be ignored safely. On the contrary, for the C diagram, because the factorizable contribution is quite small, the nonfactorizable contribution becomes significant. As it belongs to the nonperturbative contribution, we set it as universal and parametrize it as $\chi_c^C e^{i\phi_c^C}$, which will be extracted from the experimental data. In principle, the factorizable scale μ should be channel dependent; however, we find that both the fitted parameters and the predictions are not sensitive to this scale. So, for simplicity, we set $\mu = m_b/2 = 2.1$ GeV. The Wilson coefficients C_1 and C_2 at this scale are -0.287 and 1.132, respectively. As for the W-exchange E diagram, the hadronic parameter χ_c^E and its relative strong phase ϕ_c^E are also nonperturbative to be extracted from data. In practice, the dimensionless parameters χ_c^E and ϕ_c^E are defined from the $\bar{B} \to D\pi$ process, to which those for other final states are related via the ratio of the decay constants $(f_{D_{(s)}} f_P)/(f_D f_\pi)$. Obviously, the SU(3) asymmetry also remains in the E diagram. In fact, although the helicity suppression does not work with a heavy charm quark in the final state, the factorizable contribution in the E diagram is also negligible due to the smallness of the corresponding Wilson coefficient.

Similarly to the amplitudes of $\bar{B} \to DP$ decays, the topological amplitudes of T, C, and E of the $\bar{B} \to D^*P$ and $\bar{B} \to DV$ decays can be given, respectively, by

$$T_c^{D^*P} = \sqrt{2} G_F V_{cb} V_{uq}^* a_1(\mu) f_P m_{D^*} A_0^{B\to D^*}(m_P^2)(\varepsilon_{D^*}^* \cdot p_B), \tag{8}$$

$$C_c^{D^*P} = \sqrt{2} G_F V_{cb} V_{uq}^* f_{D^*} m_{D^*} F_1^{B\to P}(m_{D^*}^2) \times (\varepsilon_{D^*}^* \cdot p_B)\chi_c^C e^{i\phi_c^C}, \tag{9}$$

$$E_c^{D^*P} = \sqrt{2} G_F V_{cb} V_{uq}^* m_{D^*} f_B \frac{f_{D^*_{(s)}} f_P}{f_D f_\pi} \chi_c^E e^{i\phi_c^E}(\varepsilon_{D^*}^* \cdot p_B); \tag{10}$$

and

$$T_c^{DV} = \sqrt{2} G_F V_{cb} V_{uq}^* a_1(\mu) f_V m_V F_1^{B\to D}(m_V^2)(\varepsilon_V^* \cdot p_B), \tag{11}$$

$$C_c^{DV} = \sqrt{2} G_F V_{cb} V_{uq}^* f_D m_V A_0^{B\to V}(m_D^2)(\varepsilon_V^* \cdot p_B)\chi_c^C e^{i\phi_c^C}, \tag{12}$$

$$E_c^{DV} = \sqrt{2} G_F V_{cb} V_{uq}^* m_V f_B \frac{f_{D_{(s)}} f_V}{f_D f_\pi} \chi_c^E e^{i\phi_c^E}(\varepsilon_V^* \cdot p_B). \tag{13}$$

In the above functions, $\varepsilon_{D^*}^*$ and ε_V^* represent the polarization vectors of the D^* and V, and f_{D^*} and f_V are the decay constants of the corresponding vector mesons. $F_1^{B\to D}$ and $F_1^{B\to P}$ stand for the vector form factors of $\bar{B} \to D$ and $\bar{B} \to P$ transitions, and $A_0^{B\to D^*}$ and $A_0^{B\to V}$ are the transition form factors of $B \to D^*$ and $\bar{B} \to V$. Note that, after factorizing the corresponding form factors and decay constants, we can use the same nonperturbative universal parameters for all the $\bar{B} \to DP$, $\bar{B} \to D^*P$, and $\bar{B} \to DV$ decays. The total number of free parameters to be fitted from experimental data remains 4. This is in contrast to the conventional topological diagram approach [21], where 15 parameters are needed for the three categories of processes.

In a short summary, utilizing the factorization, the color-favored tree diagram, which is the dominant contribution in many decay channels, is determined by perturbative calculations. For the color-suppressed tree diagram and W-exchange diagram, we have only four universal nonperturbative parameters, namely, χ_c^C, ϕ_c^C, χ_c^E, and ϕ_c^E, to be fitted from all available $\bar{B} \to DP$, D^*P, and DV modes. As stated, most SU(3) breaking effects are involved in the decay constants and the transition form factors. Using the parameters determined from data, we can also reproduce branching fractions of the $\bar{B} \to DP$, D^*P, and DV modes.

B. Input parameters

In this section, we list the used parameters, such as CKM matrix elements, decay constants, and transition form factors. Since all the decay modes discussed are induced by the tree-level electroweak diagrams, we do not need the weak phases of the CKM matrix elements but use their averaged values of the magnitudes in the PDG [26]:

$$|V_{cb}| = 0.041, \qquad |V_{us}| = 0.225, \qquad |V_{ud}| = 0.974, \tag{14}$$

$$|V_{ub}| = 0.00413, \qquad |V_{cs}| = 0.986, \qquad |V_{cd}| = 0.225. \tag{15}$$

The decay constants of π, K, D, and D_s are given by the PDG [26]. The decay constants of other mesons cannot be obtained from experiments directly but calculated in several theoretical approaches, such as the quark model [27], the covariant light front approach [28], the light-cone sum rules [29,30], the QCD sum rules [31–37], the lattice QCD [38–45], etc. Since the numerical values are different in different theoretical approaches, we choose the values shown in Table I and keep a 5% uncertainty of them.

Due to the absence of enough experimental data, the transition form factors of B meson decays have been calculated in the theoretical approaches, such as the constitute quark model and light-cone quark model

TABLE I. The decay constants of mesons (in units of MeV).

f_B	f_{B_s}	f_D	f_{D_s}	f_{D^*}	$f_{D_s^*}$	f_π	f_K	f_ρ	f_{K^*}	f_ω
190	225	205	258	220	270	130	156	215	220	190

TABLE II. The transition form factors at maximum recoil and dipole model parameters used in this work.

	$F_0^{B\to\pi}$	$F_0^{B\to K}$	$F_0^{B_s\to K}$	$F_0^{B\to\eta_q}$	$F_0^{B_s\to\eta_s}$	$F_0^{B\to D}$	$F_0^{B_s\to D_s}$	$A_0^{B\to D^*}$	$A_0^{B_s\to D_s^*}$	$F_1^{B\to D}$	$F_1^{B_s\to D_s}$
$F(0)$	0.28	0.33	0.29	0.21	0.31	0.54	0.58	0.56	0.57	0.54	0.58
α_1	0.50	0.53	0.54	0.52	0.53	1.71	1.69	2.44	2.49	2.44	2.44
α_2	−0.13	−0.13	−0.15	0	0	0.52	0.78	1.98	1.74	1.49	1.70
	$F_1^{B\to\pi}$	$F_1^{B\to K}$	$F_1^{B_s\to K}$	$F_1^{B\to\eta_q}$	$F_1^{B_s\to\eta_s}$	$B_{(s)}\to V$	$A_0^{B\to\rho}$	$A_0^{B\to\omega}$	$A_0^{B_s\to\phi}$	$A_0^{B\to K^*}$	$A_0^{B_s\to K^*}$
$F(0)$	0.28	0.33	0.29	0.21	0.31	$A(0)$	0.30	0.26	0.30	0.33	0.27
α_1	0.52	0.54	0.57	1.43	1.48	α_1	1.56	1.60	1.73	1.51	1.74
α_2	0.45	0.50	0.50	0.41	0.46	α_2	0.17	0.22	0.41	0.14	0.47

[27,46–49], covariant light front approach [28,50,51], light-cone sum rules [30,52–71], PQCD [72–81], lattice QCD [82–85], etc. Considering all above results, we list the maximum-recoil form factors in Table. II. When dealing with the nonleptonic B decays, we indeed need the form factors with q^2 dependence. To describe the q^2 dependence of form factors, several types of parametrization are proposed. In the current work, we use the dipole parametrization:

$$F_i(q^2) = \frac{F_i(0)}{1-\alpha_1\frac{q^2}{m_{\rm pole}^2}+\alpha_2\frac{q^4}{m_{\rm pole}^4}}, \tag{16}$$

where F_i denotes F_0, F_1, and A_0 and $m_{\rm pole}$ is the mass of the corresponding pole state, such as B for A_0 and B^* for $F_{0,1}$. The values of α_1 and α_2 are also given in Table II. In fact, numerical results show that the q^2 dependence of form factors makes little change in our numerical calculations.

For the decay modes with η or η' in the final state, it is convenient to consider the flavor mixing of η_q and η_s, defined by

$$\eta_q = \frac{1}{\sqrt{2}}(u\bar{u}+d\bar{d}), \qquad \eta_s = s\bar{s}. \tag{17}$$

Then, η and η' are linear combinations of η_q and η_s,

$$\begin{pmatrix}\eta\\ \eta'\end{pmatrix} = \begin{pmatrix}\cos\phi & -\sin\phi\\ \sin\phi & \cos\phi\end{pmatrix}\begin{pmatrix}\eta_q\\ \eta_s\end{pmatrix}, \tag{18}$$

where the mixing angle is determined to be $\phi = (40.4\pm 0.6)^\circ$ by KLOE [86]. The flavor specific decay constants are $f_q = (1.07\pm 0.02)f_\pi$ and $f_s = (1.34\pm 0.06)f_\pi$, corresponding to η_q and η_s, respectively, [87,88]. In this work, the small effect from the mixing between ω and ϕ is ignored.

Honestly, some form factors and decay constants occur only in special channels, so their numerical values would affect the accuracy of our theoretical predictions. In this article, in order to estimate the uncertainties maximally, we shall assign the uncertainties of form factors to be 10% and the uncertainties of decay constants to be 5%. If we can determine the form factors and the decay constants more precisely by the experimental data in the future, the predicted results in the FAT approach would be improved.

C. χ^2 fit

As discussed above, there are only four parameters in the FAT approach, namely, χ^C, ϕ^C, χ^E, and ϕ^E, which are universal to all $\bar{B}\to DP$, D^*P, and DV decays. In the fitting, we define the χ^2 function in terms of n experimental observables $x_i\pm\Delta x_i$ and the corresponding theoretical predictions $x_i^{\rm th}$,

$$\chi^2 = \sum_{i=1}^{n}\left(\frac{x_i^{\rm th}-x_i}{\Delta x_i}\right)^2. \tag{19}$$

In this work, the data points are the branching fractions. We then write the corresponding theoretical predictions in terms of topological amplitudes and extract the four parameters by minimizing χ^2. Currently, there are 31 experimental measured charmed decay modes induced by $b\to c$ transition [26]. With these data, the best-fitted values of the parameters are obtained as

$$\begin{aligned}\chi_c^C &= 0.48\pm 0.01, \qquad & \phi_c^C &= (56.6^{+3.2}_{-3.8})^\circ,\\ \chi_c^E &= 0.024^{+0.002}_{-0.001}, \qquad & \phi_c^E &= (123.9^{+3.3}_{-2.2})^\circ,\end{aligned} \tag{20}$$

with $\chi^2/{\rm d.o.f.} = 1.4$.

In Ref. [21], Chiang *et al.* fitted the amplitudes and strong phases of each diagram using the latest experimental data in the topological diagram approach. Because they do not include the SU(3) breaking effects properly, they had to fit each amplitude of $B\to DP$, DV, and D^*P decays separately. Even though with much more parameters than us, their χ^2 per degree of freedom is larger than ours. Only under the so-called scheme 3, where totally 21 parameters have been fitted from data for involving the SU(3) symmetry breaking effects, their χ^2/d.o.f. for the $B\to DP$ decays is a little smaller than ours. But the χ^2/d.o.f. for the $B\to DV$ and D^*P decays is still larger than ours. With so many parameters, they lost the predictive power of the branching fractions because there are not enough data of the $B\to\bar{D}^{(*)}M$ decays. By contrast, we can predict 120 branching fractions, by fitting four parameters from 31 decay modes.

D. Branching fractions

With the fitted parameters, the topological amplitudes and the predicted branching fractions of $\bar{B}\to DP$, D^*P,

TABLE III. Branching fractions and decay amplitudes for the $\bar{B} \to DP$ modes. Data are from Ref. [26]. The first uncertainties are from the fitted parameters, the second uncertainties are from the form factors, and the third ones are coming from decay constants.

Meson	Mode	Amplitudes	$\mathcal{B}_{\rm exp}(\times 10^{-4})$	$\mathcal{B}_{\rm th}(\times 10^{-4})$
	Cabibbo favored	$V_{cb}V_{ud}^*$		
$\bar{B}^0$	$D^+\pi^-$	$T+E$	26.8 ± 1.3	$24.7^{+0.2}_{-0.1} \pm 5.1 \pm 0.1$
	$D^0\pi^0$	$\frac{1}{\sqrt{2}}(E-C)$	2.63 ± 0.14	$2.5^{+0.1}_{-0.2} \pm 0.5 \pm 0.1$
	$D^0\eta$	$\frac{1}{\sqrt{2}}(C+E)\cos\phi$	2.36 ± 0.32	$1.9 \pm 0.1 \pm 0.4 \pm 0.1$
	$D^0\eta'$	$\frac{1}{\sqrt{2}}(C+E)\sin\phi$	1.38 ± 0.16	$1.3 \pm 0.1 \pm 0.2 \pm 0.1$
	$D_s^+K^-$	E	0.345 ± 0.032	$0.30^{+0.04}_{-0.02} \pm 0.00 \pm 0.03$
B^-	$D^0\pi^-$	$T+C$	48.1 ± 1.5	$49.0^{+1.4}_{-1.7} \pm 7.6 \pm 0.6$
$\bar{B}_s^0$	$D_s^+\pi^-$	T	30.4 ± 2.3	$30.2 \pm 0.0 \pm 6.0 \pm 0.1$
	D^0K^0	C		$5.9 \pm 0.3 \pm 1.2 \pm 0.3$
	Cabibbo suppressed	$V_{cb}V_{us}^*$		
$\bar{B}^0$	D^+K^-	T	1.97 ± 0.21	$2.1 \pm 0.0 \pm 0.4 \pm 0.0$
	$D^0\bar{K}^0$	C	0.52 ± 0.07	$0.4 \pm 0.0 \pm 0.1 \pm 0.0$
B^-	D^0K^-	$T+C$	3.70 ± 0.17	$3.8 \pm 0.1 \pm 0.6 \pm 0.1$
$\bar{B}_s^0$	$D_s^+K^-$	$T+E$		$2.1 \pm 0.0 \pm 0.4 \pm 0.0$
	$D^0\eta$	$\frac{1}{\sqrt{2}}E\cos\phi - C\sin\phi$		$0.14 \pm 0.01 \pm 0.03 \pm 0.01$
	$D^0\eta'$	$\frac{1}{\sqrt{2}}E\sin\phi + C\cos\phi$		$0.21 \pm 0.01 \pm 0.04 \pm 0.01$
	$D^+\pi^-$	E		$0.011 \pm 0.001 \pm 0.000 \pm 0.001$
	$D^0\pi^0$	$\frac{1}{\sqrt{2}}E$		$0.005^{+0.001}_{-0.000} \pm 0.000 \pm 0.001$

and DV decays induced by $b \to c$ transition are shown in Tables III, IV, and V, respectively. The experimental data are also given for comparison. For all theoretical predictions, the first uncertainties arise from the aforementioned four parameters fitted in the FAT approach. The second uncertainties come from the transition form factors, and the third ones are from decay constants. From the tables, it is obvious that the major uncertainties are from form factors. Moreover, we note that each table is divided into two parts, Cabibbo favored (V_{ud} or V_{cs}) and Cabibbo suppressed (V_{us} or V_{cd}), and most branching fractions of the Cabibbo-favored processes are larger than those of Cabibbo-suppressed ones.

TABLE IV. Branching fractions and decay amplitudes for the $\bar{B} \to D^*P$ decays.

Meson	Mode	Amplitudes	$\mathcal{B}_{\rm exp}(\times 10^{-4})$	$\mathcal{B}_{\rm th}(\times 10^{-4})$
	Cabibbo favored	$V_{cb}V_{ud}^*$		
$\bar{B}^0$	$D^{*+}\pi^-$	$T+E$	27.6 ± 1.3	$24.9^{+0.2}_{-0.1} \pm 5.2 \pm 0.1$
	$D^{*0}\pi^0$	$\frac{1}{\sqrt{2}}(E-C)$	2.2 ± 0.6	$2.8 \pm 0.2 \pm 0.6 \pm 0.3$
	$D^{*0}\eta$	$\frac{1}{\sqrt{2}}(C+E)\cos\phi$	2.3 ± 0.6	$2.1 \pm 0.1 \pm 0.4 \pm 0.2$
	$D^{*0}\eta'$	$\frac{1}{\sqrt{2}}(C+E)\sin\phi$	1.40 ± 0.22	$1.4 \pm 0.1 \pm 0.2 \pm 0.1$
	$D_s^{*+}K^-$	E	0.219 ± 0.030	$0.22^{+0.03}_{-0.01} \pm 0.00 \pm 0.03$
B^-	$D^{*0}\pi^-$	$T+C$	51.8 ± 2.6	$50.7^{+1.5}_{-1.8} \pm 7.8 \pm 1.4$
$\bar{B}_s^0$	$D_s^{*+}\pi^-$	T	20 ± 5	$27.1 \pm 0.0 \pm 5.4 \pm 0.1$
	$D^{*0}K^0$	C		$6.6^{+0.3}_{-0.4} \pm 1.3 \pm 0.7$
	Cabibbo suppressed	$V_{cb}V_{us}^*$		
$\bar{B}^0$	$D^{*+}K^-$	T	2.14 ± 0.16	$2.0 \pm 0.00 \pm 0.4 \pm 0.0$
	$D^{*0}\bar{K}^0$	C	0.36 ± 0.12	$0.45^{+0.02}_{-0.03} \pm 0.09 \pm 0.05$
B^-	$D^{*0}K^-$	$T+C$	4.20 ± 0.34	$3.8 \pm 0.1 \pm 0.6 \pm 0.1$
$\bar{B}_s^0$	$D_s^{*+}K^-$	$T+E$		$1.9 \pm 0.0 \pm 0.4 \pm 0.0$
	$D^{*0}\eta$	$\frac{1}{\sqrt{2}}E\cos\phi - C\sin\phi$		$0.15 \pm 0.01 \pm 0.03 \pm 0.02$
	$D^{*0}\eta'$	$\frac{1}{\sqrt{2}}E\sin\phi + C\cos\phi$		$0.23 \pm 0.01 \pm 0.04 \pm 0.02$
	$D^{*+}\pi^-$	E	< 0.061	$0.009 \pm 0.001 \pm 0.000 \pm 0.001$
	$D^{*0}\pi^0$	$\frac{1}{\sqrt{2}}E$		$0.004^{+0.004}_{-0.000} \pm 0.000 \pm 0.001$

TABLE V. Branching fractions and decay amplitudes for the $\bar{B} \to DV$ decays.

Meson	Mode	Amplitudes	$\mathcal{B}_{\rm exp}(\times 10^{-4})$	$\mathcal{B}_{\rm th}(\times 10^{-4})$
	Cabibbo favored	$V_{cb}V_{ud}^*$		
$\bar{B}^0$	$D^+\rho^-$	$T+E$	78 ± 13	$65.3^{+0.5}_{-0.3} \pm 13.5 \pm 6.6$
	$D^0\rho^0$	$\frac{1}{\sqrt{2}}(E-C)$	3.2 ± 0.5	$2.6 \pm 0.2 \pm 0.6 \pm 0.1$
	$D^0\omega$	$\frac{1}{\sqrt{2}}(E+C)$	2.54 ± 0.16	$2.7 \pm 0.2 \pm 0.5 \pm 0.1$
	$D_s^+K^{*-}$	E	0.35 ± 0.10	$0.38^{+0.05}_{-0.02} \pm 0.00 \pm 0.06$
B^-	$D^0\rho^-$	$T+C$	134 ± 18	$105^{+2}_{-3} \pm 18 \pm 9$
$\bar{B}_s^0$	$D_s^+\rho^-$	T	70 ± 15	$78.6 \pm 0.0 \pm 15.7 \pm 7.9$
	D^0K^{*0}	C	3.5 ± 0.6	$4.9^{+0.2}_{-0.3} \pm 1.0 \pm 0.2$
	Cabibbo suppressed	$V_{cb}V_{us}^*$		
$\bar{B}^0$	D^+K^{*-}	T	4.5 ± 0.7	$3.9 \pm 0.0 \pm 0.8 \pm 0.4$
	$D^0\bar{K}^{*0}$	C	0.42 ± 0.06	$0.37 \pm 0.02 \pm 0.07 \pm 0.02$
B^-	D^0K^{*-}	$T+C$	5.3 ± 0.4	$6.0^{+0.1}_{-0.2} \pm 1.0 \pm 0.5$
$\bar{B}_s^0$	$D_s^+K^{*-}$	$T+E$		$4.0^{+0.04}_{-0.03} \pm 0.8 \pm 0.4$
	$D^0\phi$	C	0.24 ± 0.07	$0.31^{+0.01}_{-0.02} \pm 0.06 \pm 0.02$
	$D^+\rho^-$	E		$0.019^{+0.002}_{-0.001} \pm 0.000 \pm 0.003$
	$D^0\rho^0$	$\frac{1}{\sqrt{2}}E$		$0.010 \pm 0.001 \pm 0.000 \pm 0.001$
	$D^0\omega$	$\frac{1}{\sqrt{2}}E$		$0.008 \pm 0.001 \pm 0.000 \pm 0.001$

From the tables, we find that our results are consistent with the measured B^- and $\bar{B}^0$ decays induced by $b \to c$ transition. As for $\bar{B}_s^0$, only a few typical decays, such as $\bar{B}_s^0 \to D_s^{(*)+}\pi^-$, have been measured in the LHCb, while most of them will be tested in the LHCb in the following years. Comparing with Ref. [21], most of the results are in agreement with each other.

In Tables III, IV, and V, for the decays dominated by the T diagram, because the decay constants of light vector mesons are much larger than those of light pseudoscalar ones, the branching fractions of the $\bar{B} \to DV$ decays are larger than those of the $\bar{B} \to DP$ and $\bar{B} \to D^*P$ with a light meson emitted. For example, the branching fractions of $\bar{B}^0 \to D^+\rho^-$ are larger than those of $\bar{B}^0 \to D^{(*)+}\pi^-$ by a factor of 2.6 because of $f_\rho > f_\pi$. Similarly, we obtain $\mathcal{B}(\bar{B}^0 \to D^+K^{*-}) > \mathcal{B}(\bar{B}^0 \to D^{(*)+}K^-)$, $\mathcal{B}(\bar{B}_s^0 \to D_s^+\rho^-) > \mathcal{B}(\bar{B}_s^0 \to D_s^{(*)+}\pi^-)$, and $\mathcal{B}(\bar{B}_s^0 \to D_s^+K^{*-}) > \mathcal{B}(\bar{B}_s^0 \to D_s^{(*)+}K^-)$. For the D^*P modes, there is no contribution of transverse polarizations, and the behavior of the longitudinal polarization is similar to that of the pseudoscalar meson, so the branching fractions of $\bar{B} \to D^*P$ are close to those of $\bar{B} \to DP$.

Compared with the QCD-inspired methods [9,11,18,19], the amplitudes of color-suppressed C diagrams are relatively large in the FAT approach where the nonfactorizable contributions are dominant, and this conclusion has been also confirmed in the topological approach [21]. From Table III, it is found that the branching fraction of $\bar{B}^0 \to D^+\pi^-$ is larger than that of $\bar{B}^0 \to D_s^+K^-$ by 2 orders of magnitude, which implies that the contribution of the E diagram is much smaller than that of the T diagram. So, the E diagram can be neglected as a good approximation in the processes with both T and E contributions. In the comparison between the $\bar{B}^0 \to D^+K^-$ with $\bar{B}^0 \to D^0\bar{K}^0$, and $\bar{B}_s^0 \to D_s^+\pi^-$ with $\bar{B}_s^0 \to D^0K^0$, we find that

$$|C_c^{DP}|/|T_c^{DP}| \sim 0.45. \tag{21}$$

Then, the hierarchy

$$|T_c^{DP}|:|C_c^{DP}|:|E_c^{DP}| \sim 1:0.45:0.1 \tag{22}$$

is obtained in the FAT approach. Similarly, we also get

$$|T_c^{D^*P}|:|C_c^{D^*P}|:|E_c^{D^*P}| \sim 1:0.36:0.1 \tag{23}$$

$$|T_c^{DV}|:|C_c^{DV}|:|E_c^{DV}| \sim 1:0.31:0.1. \tag{24}$$

It is obvious that these relations differ from the relation $|T_c^{DP}| \gg |C_c^{DP}| \sim |E_c^{DP}|$ arrived at in the PQCD approach [18] and have significant impacts on the processes without T diagrams. For example, the topological amplitudes of $\bar{B}^0 \to D^0\rho^0$ and $D^0\omega$ decays are $(E-C)/\sqrt{2}$ and $(E+C)/\sqrt{2}$, respectively. The branching fraction of the $D^0\rho^0$ mode is predicted to be almost one-half of that of the $D^0\omega$ mode in the PQCD approach [18], since C and E diagrams contribute destructively for the former mode but constructively for the latter one, which does not agree with the experiment. However, this issue can be easily explained in the FAT approach in which both channels are dominated by the C diagram. With the same argument, the experimental data of the decay modes $\bar{B}_d^0 \to D^0\pi^0$ and $D^0\bar{K}^0$ can be easily understood.

III. CKM-SUPPRESSED DECAYS INDUCED BY $b \to u$ TRANSITION

In this section, we shall study the CKM-suppressed processes induced by $b \to u\bar{c}d(s)$ transitions, i.e., $\bar{B} \to \bar{D}P$, $\bar{D}^*P$, and $\bar{D}V$ decay modes. The relevant effective Hamiltonian can be obtained by an exchange of $c \leftrightarrow u$ in that of the $b \to c$ transiting processes shown in Eq. (2), as

$$\mathcal{H}_{\rm eff} = \frac{G_F}{\sqrt{2}} V_{ub}V_{cq}^*[C_1(\mu)O_1(\mu) + C_2(\mu)O_2(\mu)] + \text{H.c.}, \tag{25}$$

where the two tree-level current-current operators are

$$\begin{aligned} O_1 &= \bar{q}_\alpha \gamma^\mu(1-\gamma_5)c_\beta \bar{u}_\beta \gamma_\mu(1-\gamma_5)b_\alpha, \\ O_2 &= \bar{q}_\alpha \gamma^\mu(1-\gamma_5)c_\alpha \bar{u}_\beta \gamma_\mu(1-\gamma_5)b_\beta. \end{aligned} \tag{26}$$

According the effective Hamiltonian, we can draw the topological diagrams of the $b \to u$ transitions as shown in Fig. 2.

The topologies of the processes $\bar{B} \to \bar{D}^{(*)}M$ induced by $b \to u$ transition are different from $\bar{B} \to D^{(*)}M$ induced by $b \to c$. The charmed meson is recoiled in $\bar{B} \to D^{(*)}M$, while it will be emitted in the $\bar{B} \to \bar{D}^{(*)}M$ process. It is thus expected that the branching fractions of $\bar{B} \to \bar{D}^{(*)}M$ are smaller than those of $\bar{B} \to D^{(*)}M$ due to the suppression of CKM elements. The formulas of $\bar{B} \to \bar{D}^{(*)}M$ factorizable contributions should be similar to those of $\bar{B} \to D^{(*)}M$, but four new nonfactorizable contributions, i.e., $\chi_u^{C,E}$ and $\phi_u^{C,E}$, should be introduced. In principle, these parameters should be extracted from experimental data as done in the $b \to c$ processes, but there are no C- or E-diagram dominated modes measured in the experiments so far. In this case, we shall employ an approximation that the four nonfactorizable parameters in the $b \to u$ processes are the same as those in the $b \to c$ processes. Therefore, the formulas of the T, C, and E diagrams are the same in these two kinds of processes, i.e., $\chi_u^C = \chi_c^C$, $\phi_u^C = \phi_c^C$, $\chi_u^E = \chi_c^E$, and $\phi_u^E = \phi_c^E$. In the following, we will neglect the subscripts of $\chi_{u,c}^{C,E}$ and $\phi_{u,c}^{C,E}$ for simplicity without confusion.

Apart from the above contributions, the W-annihilation diagram A appears in the $b \to u$ transitions. Again, no experimental data are available to fit the contribution of this diagram. Unlike the E diagram dominated by nonfactorizable contributions, the factorizable contributions in the A diagram are too large to be neglected. On the contrary, the nonfactorizable contributions are suppressed due to the small Wilson coefficient $C_1/3$. To calculate the factorizable contribution in the A diagram quantitatively, we will adopt the pole model [22,23,89,90], which has been proven to be one effective approach in dealing with the W-annihilation diagrams. So, the amplitudes are expressed as

$$A_u^{DP} = -i\frac{G_F}{\sqrt{2}} V_{ub}V_{cq}^* \left(C_2(\mu) + \frac{C_1(\mu)}{N_c}\right) f_B \frac{f_{D_0^*} g_{D_0^* DP} m_{D_0^*}^3}{m_B^2 - m_{D_0^*}^2}, \tag{27}$$

$$A_u^{D^*P} = \sqrt{2}G_F V_{ub}V_{cq}^* \left(C_2(\mu) + \frac{C_1(\mu)}{N_c}\right) \times f_B \frac{f_D g_{D^*DP} m_D^2}{m_B^2 - m_D^2}(\varepsilon_{D^*}^* \cdot p_B), \tag{28}$$

$$A_u^{DV} = \sqrt{2}G_F V_{ub}V_{cq}^* \left(C_2(\mu) + \frac{C_1(\mu)}{N_c}\right) \times f_B \frac{f_D g_{DDV} m_D^2}{m_B^2 - m_D^2}(\varepsilon_V^* \cdot p_B), \tag{29}$$

where the intermediate state is a scalar charmed meson D_0 in the $\bar{D}P$ mode and a pseudoscalar D meson in the $\bar{D}^*P$ and $\bar{D}V$ modes. The effective strong coupling constant $g_{D_0^*DP} = 4.2$ is extracted from the experimental data of $D_0^*(2400) \to D\pi$ decay, $g_{D^*DP} = 4.8$ is from $D^* \to D\pi$ decay [26], and $g_{DDV} = 2.52$ is obtained from the vector meson dominance model [91]. In practice, we will follow the arguments of Ref. [89] to set all intermediate states on shell, i.e., $p_{\rm pole}^2 = m_{\rm pole}^2$, for simplicity.

With the fitted parameters from processions induced by $b \to c$ transition, the topological amplitudes and the predicted branching fractions of processes induced by $b \to u$ transition are tabled in Tables VI, VII, and VIII. In these three tables, the resources of the first three uncertainties are the same as processes induced by the

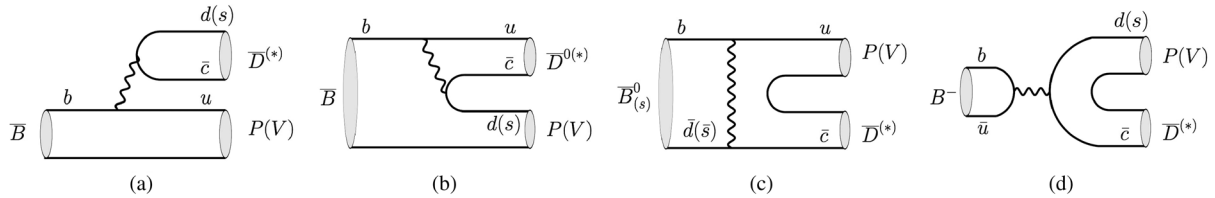

FIG. 2. Topological diagrams in the $b \to u$ transitions: (a) the color-favored tree diagram, T; (b) the colorsuppressed tree diagram, C; (c) the W-exchange annihilation-type diagram, E; and (d) the W-annihilation diagram, A. Note that the E diagram occurs only in the $\bar{B}_d^0$ and $\bar{B}_s^0$ decays, while the A diagram occurs only in B^- decays.

TABLE VI. Branching fractions and decay amplitudes for the $\bar{B} \to \bar{D}P$ modes. Data are from Ref. [26]. The first uncertainties are from the fitted parameters, the second uncertainties are from the form factors, the third ones are coming from decay constants, and the last ones are from $|V_{ub}|$.

Meson	Mode	Amplitudes	$\mathcal{B}_{\rm exp}(\times 10^{-6})$	$\mathcal{B}_{\rm th}(\times 10^{-6})$
	Cabibbo favored	$V_{ub}V_{cs}^*$		
$\bar{B}^0$	$D_s^-\pi^+$	T	21.6 ± 2.6	$29.1 \pm 0.0 \pm 6.3 \pm 1.0 \pm 7.0$
	$\bar{D}^0\bar{K}^0$	C		$5.7 \pm 0.3 \pm 1.2 \pm 0.3 \pm 1.4$
B^-	$D_s^-\pi^0$	$\frac{1}{\sqrt{2}}T$	16 ± 5	$15.6 \pm 0.0 \pm 3.4 \pm 0.6 \pm 3.8$
	$D_s^-\eta$	$\frac{1}{\sqrt{2}}T\cos\phi$	< 400	$9.8 \pm 0.0 \pm 2.0 \pm 0.3 \pm 2.4$
	$D_s^-\eta'$	$\frac{1}{\sqrt{2}}T\sin\phi$		$5.9 \pm 0.0 \pm 1.3 \pm 0.2 \pm 1.4$
	$\bar{D}^0K^-$	$C + A$		$5.8 \pm 0.3 \pm 1.3 \pm 0.3 \pm 1.4$
	$D^-\bar{K}^0$	A	< 2.9	$0.012 \pm 0.000 \pm 0.000 \pm 0.000 \pm 0.003$
$\bar{B}_s^0$	$D_s^-K^+$	$T + E$		$27.5^{+0.3}_{-0.2} \pm 6.6 \pm 1.0 \pm 6.6$
	$\bar{D}^0\eta$	$\frac{1}{\sqrt{2}}E\cos\phi - C\sin\phi$		$2.0 \pm 0.1 \pm 0.4 \pm 0.1 \pm 0.5$
	$\bar{D}^0\eta'$	$\frac{1}{\sqrt{2}}E\sin\phi + C\cos\phi$		$2.9 \pm 0.1 \pm 0.6 \pm 0.1 \pm 0.7$
	$D^-\pi^+$	E		$0.14 \pm 0.02 \pm 0.00 \pm 0.02 \pm 0.03$
	$\bar{D}^0\pi^0$	$\frac{1}{\sqrt{2}}E$		$0.07 \pm 0.01 \pm 0.00 \pm 0.01 \pm 0.02$
	Cabibbo suppressed	$V_{ub}V_{cd}^*$		
$\bar{B}^0$	$D^-\pi^+$	$T + E$	0.78 ± 0.14	$0.90 \pm 0.01 \pm 0.20 \pm 0.04 \pm 0.22$
	$\bar{D}^0\pi^0$	$\frac{1}{\sqrt{2}}(E - C)$		$0.11 \pm 0.01 \pm 0.02 \pm 0.01 \pm 0.03$
	$\bar{D}^0\eta$	$\frac{1}{\sqrt{2}}(E + C)\cos\phi$		$0.07 \pm 0.01 \pm 0.01 \pm 0.00 \pm 0.02$
	$\bar{D}^0\eta'$	$\frac{1}{\sqrt{2}}(E + C)\sin\phi$		$0.05 \pm 0.00 \pm 0.01 \pm 0.00 \pm 0.01$
	$D_s^-K^+$	E		$0.011 \pm 0.001 \pm 0.000 \pm 0.001 \pm 0.003$
B^-	$\bar{D}^0\pi^-$	$C + A$		$0.23 \pm 0.01 \pm 0.05 \pm 0.01 \pm 0.05$
	$D^-\pi^0$	$\frac{1}{\sqrt{2}}(T - A)$		$0.55 \pm 0.00 \pm 0.12 \pm 0.03 \pm 0.13$
	$D^-\eta$	$\frac{1}{\sqrt{2}}(T + A)\cos\phi$		$0.30 \pm 0.00 \pm 0.06 \pm 0.02 \pm 0.07$
	$D^-\eta'$	$\frac{1}{\sqrt{2}}(T + A)\sin\phi$		$0.20 \pm 0.00 \pm 0.04 \pm 0.01 \pm 0.05$
	$D_s^-K^0$	A	< 800	$0.0006 \pm 0.0000 \pm 0.0000 \pm 0.0001 \pm 0.0002$
$\bar{B}_s^0$	D^-K^+	T		$1.05 \pm 0.00 \pm 0.24 \pm 0.05 \pm 0.25$
	$\bar{D}^0K^0$	C		$0.24 \pm 0.01 \pm 0.05 \pm 0.01 \pm 0.06$

$b \to c$ transition. Besides, we also include the uncertainties arising from the CKM matrix element $|V_{ub}|$, which has not been well measured till now. From the tables, it is obvious that both form factors and $|V_{ub}|$ take large uncertainties. If the CKM matrix element $|V_{ub}|$ can be determined well, it is expected that the uncertainties from it will be reduced significantly. It should be noted that the decays by $b \to u$ transitions should have additional uncertainties compared to decay by $b \to c$ transition, since our approximation of the same parameters for these two kinds of decays are not well justified. Similarly, we also obtain the hierarchy $|T_u|:|C_u|:|E_u|:|A_u| \sim 1:0.4:0.1:0.03$. Compared with some existing data, our predictions are in agreement with them with large uncertainties on both sides. And these results will be tested in the LHCb and Belle-II experiments. Note that the branching fractions of the processes induced only by the W-annihilation diagram are so small that they can be regarded as the good place to probe new physics beyond the SM, though these predictions in the current work are somewhat model dependent.

IV. PHENOMENOLOGICAL IMPLICATIONS

In this section, we are going to discuss the isospin asymmetry, SU(3), and CP asymmetry in turn.

A. Isospin analysis

The $\bar{B} \to D\pi$ system can be decomposed in terms of two isospin amplitudes, $A_{1/2}$ and $A_{3/2}$, which correspond to the transition into $D\pi$ final states with isospin $I = 1/2$ and $I = 3/2$, respectively. In the experimental side, the ratio

$$\frac{A_{1/2}}{\sqrt{2}A_{3/2}} = 1 + \mathcal{O}(\Lambda_{\rm QCD}/m_b) \tag{30}$$

is a measure of the departure from the heavy-quark limit [59]. The corresponding isospin relations read as

$$A(\bar{B}_d^0 \to D^+\pi^-) = \sqrt{\frac{1}{3}}A_{3/2} + \sqrt{\frac{2}{3}}A_{1/2} = T + E, \tag{31a}$$

TABLE VII. Branching fractions and decay amplitudes for the $\bar{B} \to \bar{D}^* P$ decays.

Meson	Mode	Amplitudes	$\mathcal{B}_{\rm exp}(\times 10^{-6})$	$\mathcal{B}_{\rm th}(\times 10^{-6})$
	Cabibbo favored	$V_{ub}V_{cs}^*$		
$\bar{B}^0$	$D_s^{*-}\pi^+$	T	21 ± 4	$31.0 \pm 0.0 \pm 6.6 \pm 3.1 \pm 7.4$
	$\bar{D}^{*0}\bar{K}^0$	C		$6.4 \pm 0.3 \pm 1.4 \pm 0.6 \pm 1.5$
B^-	$D_s^{*-}\pi^0$	$\frac{1}{\sqrt{2}}T$	< 260	$16.6 \pm 0.0 \pm 3.6 \pm 1.7 \pm 4.0$
	$D_s^{*-}\eta$	$\frac{1}{\sqrt{2}}T\cos\phi$	< 600	$6.0 \pm 0.0 \pm 1.6 \pm 0.8 \pm 1.4$
	$D_s^{*-}\eta'$	$\frac{1}{\sqrt{2}}T\sin\phi$		$10.7 \pm 0.0 \pm 1.7 \pm 0.9 \pm 2.6$
	$\bar{D}^{*0}K^-$	$C + A$		$11.8^{+0.5}_{-0.6} \pm 1.9 \pm 0.9 \pm 2.8$
	$D^{*-}\bar{K}^0$	A	< 9.0	$1.3 \pm 0.0 \pm 0.0 \pm 0.1 \pm 0.3$
$\bar{B}_s^0$	$D_s^{*-}K^+$	$T + E$		$29.7^{+0.3}_{-0.2} \pm 7.1 \pm 3.0 \pm 7.1$
	$\bar{D}^{*0}\eta$	$\frac{1}{\sqrt{2}}E\cos\phi - C\sin\phi$		$2.3 \pm 0.1 \pm 0.5 \pm 0.2 \pm 0.6$
	$\bar{D}^{*0}\eta'$	$\frac{1}{\sqrt{2}}E\sin\phi + C\cos\phi$		$3.1 \pm 0.1 \pm 0.6 \pm 0.3 \pm 0.8$
	$D^{*-}\pi^+$	E		$0.11 \pm 0.01 \pm 0.00 \pm 0.02 \pm 0.03$
	$\bar{D}^{*0}\pi^0$	$\frac{1}{\sqrt{2}}E$		$0.06 \pm 0.01 \pm 0.00 \pm 0.01 \pm 0.01$
	Cabibbo suppressed	$V_{ub}V_{cd}^*$		
$\bar{B}^0$	$D^{*-}\pi^+$	$T + E$		$1.0 \pm 0.0 \pm 0.2 \pm 0.1 \pm 0.2$
	$\bar{D}^{*0}\pi^0$	$\frac{1}{\sqrt{2}}(E - C)$		$0.12 \pm 0.01 \pm 0.03 \pm 0.01 \pm 0.03$
	$\bar{D}^{*0}\eta$	$\frac{1}{\sqrt{2}}(E + C)\cos\phi$		$0.08 \pm 0.0 \pm 0.02 \pm 0.02 \pm 0.02$
	$\bar{D}^{*0}\eta'$	$\frac{1}{\sqrt{2}}(E + C)\sin\phi$		$0.05 \pm 0.0 \pm 0.01 \pm 0.00 \pm 0.01$
	$D_s^{*-}K^+$	E		$0.008 \pm 0.001 \pm 0.000 \pm 0.001 \pm 0.002$
B^-	$\bar{D}^{*0}\pi^-$	$C + A$		$0.43 \pm 0.02 \pm 0.07 \pm 0.03 \pm 0.10$
	$D^{*-}\pi^0$	$\frac{1}{\sqrt{2}}(T - A)$	< 3.6	$0.40 \pm 0.00 \pm 0.11 \pm 0.05 \pm 0.10$
	$D^{*-}\eta$	$\frac{1}{\sqrt{2}}(T + A)\cos\phi$		$0.48 \pm 0.00 \pm 0.09 \pm 0.04 \pm 0.12$
	$D^{*-}\eta'$	$\frac{1}{\sqrt{2}}(T + A)\sin\phi$		$0.31 \pm 0.00 \pm 0.06 \pm 0.03 \pm 0.07$
	$D_s^{*-}K^0$	A	< 900	$0.03 \pm 0.00 \pm 0.00 \pm 0.00 \pm 0.01$
$\bar{B}_s^0$	$D^{*-}K^+$	T		$1.17 \pm 0.00 \pm 0.27 \pm 0.12 \pm 0.28$
	$\bar{D}^{*0}K^0$	C		$0.27 \pm 0.01 \pm 0.06 \pm 0.03 \pm 0.06$

$$\sqrt{2}A(\bar{B}_d^0 \to D^0\pi^0) = \sqrt{\frac{4}{3}}A_{3/2} - \sqrt{\frac{2}{3}}A_{1/2} = C - E, \quad (31b)$$

$$A(B_u^- \to D^0\pi^-) = \sqrt{3}A_{3/2} = T + C. \quad (31c)$$

So, the isospin amplitudes can be expressed by the topological amplitudes as

$$A_{1/2} = \frac{2T - C + 3E}{\sqrt{6}}, \qquad A_{3/2} = \frac{T + C}{\sqrt{3}}, \quad (32)$$

which leads to the following expression:

$$\frac{A_{1/2}}{\sqrt{2}A_{3/2}} = 1 - \frac{3}{2}\left(\frac{C - E}{T + C}\right). \quad (33)$$

The relative strong phase between the $I = 3/2$ and $I = 1/2$ amplitudes can be calculated with

$$\cos\delta = \frac{3|A(D^+\pi^-)|^2 + |A(D^0\pi^-)|^2 - 6|A(D^0\pi^0)|^2}{6\sqrt{2}|A_{1/2}||A_{3/2}|}. \quad (34)$$

In this work, we find the following numerical results:

$$\left|\frac{A_{1/2}}{\sqrt{2}A_{3/2}}\right|_{D\pi} = 0.65 \pm 0.03, \quad (35)$$

which are complemented by

$$\cos\delta = 0.90 \pm 0.04. \quad (36)$$

The corresponding central values for the strong phases then become $\delta = 25°$. Comparing with Eq. (30), we observe that the isospin-amplitude ratio shows significant deviation from the heavy-quark limit. Because the contribution from annihilations has been neglected, we can trace this feature back to the large color-suppressed C topologies.

B. SU(3) symmetry breaking

Now, we turn to discuss the SU(3) symmetry breaking effect in the charmed B decays. If flavor SU(3) were exact, one would get:

TABLE VIII. Branching fractions and decay amplitudes for the $\bar{B} \to \bar{D}V$ decays.

Meson	Mode	Amplitudes	$\mathcal{B}_{\rm exp}(\times 10^{-6})$	$\mathcal{B}_{\rm th}(\times 10^{-6})$
	Cabibbo favored	$V_{ub}V_{cs}^*$		
$\bar{B}^0$	$D_s^-\rho^+$	T	< 24	$31.2 \pm 0.0 \pm 7.5 \pm 1.1 \pm 7.5$
	$\bar{D}^0\bar{K}^{*0}$	C	< 11	$5.2 \pm 0.3 \pm 1.2 \pm 0.2 \pm 1.2$
B^-	$D_s^-\rho^0$	$\frac{1}{\sqrt{2}}T$	< 300	$16.8 \pm 0.0 \pm 4.0 \pm 0.6 \pm 4.0$
	$D_s^-\omega$	$\frac{1}{\sqrt{2}}T$	< 400	$12.7 \pm 0.0 \pm 3.1 \pm 0.5 \pm 3.1$
	$\bar{D}^0K^{*-}$	$C + A$		$11.2^{+0.5}_{-0.6} \pm 1.7 \pm 0.5 \pm 2.7$
	$D^-\bar{K}^{*0}$	A	< 1.8	$1.8 \pm 0.0 \pm 0.0 \pm 0.2 \pm 0.4$
	$D_s^-\phi$	A	$1.7^{+1.2}_{-0.7}$	$1.2 \pm 0.0 \pm 0.0 \pm 0.1 \pm 0.3$
$\bar{B}_s^0$	$D_s^-K^{*+}$	$T + E$		$22.4^{+0.3}_{-0.2} \pm 4.3 \pm 0.8 \pm 5.4$
	$\bar{D}^0\phi$	C		$4.4 \pm 0.2 \pm 1.1 \pm 0.2 \pm 1.1$
	$D^-\rho^+$	E		$0.25^{+0.03}_{-0.01} \pm 0.00 \pm 0.04 \pm 0.06$
	$\bar{D}^0\rho^0$	$\frac{1}{\sqrt{2}}E$		$0.13^{+0.02}_{-0.01} \pm 0.00 \pm 0.02 \pm 0.03$
	$\bar{D}^0\omega$	$\frac{1}{\sqrt{2}}E$		$0.11 \pm 0.01 \pm 0.00 \pm 0.02 \pm 0.03$
	Cabibbo suppressed	$V_{ub}V_{cd}^*$		
$\bar{B}^0$	$D^-\rho^+$	$T + E$		$0.94 \pm 0.01 \pm 0.24 \pm 0.05 \pm 0.22$
	$\bar{D}^0\rho^0$	$\frac{1}{\sqrt{2}}(E - C)$		$0.12 \pm 0.01 \pm 0.03 \pm 0.01 \pm 0.03$
	$\bar{D}^0\omega$	$\frac{1}{\sqrt{2}}(E + C)$		$0.10 \pm 0.01 \pm 0.02 \pm 0.01 \pm 0.02$
	$D_s^-K^{*+}$	E		$0.014^{+0.002}_{-0.001} \pm 0.000 \pm 0.002 \pm 0.003$
B^-	$D^-\rho^0$	$\frac{1}{\sqrt{2}}(T - A)$		$0.33 \pm 0.00 \pm 0.10 \pm 0.02 \pm 0.08$
	$D^-\omega$	$\frac{1}{\sqrt{2}}(T + A)$		$0.69 \pm 0.00 \pm 0.13 \pm 0.04 \pm 0.17$
	$\bar{D}^0\rho^-$	$C + A$		$0.48 \pm 0.02 \pm 0.08 \pm 0.02 \pm 0.11$
	$D_s^-K^{*0}$	A	< 4.4	$0.04 \pm 0.00 \pm 0.00 \pm 0.01 \pm 0.01$
$\bar{B}_s^0$	D^-K^{*+}	T		$0.88 \pm 0.00 \pm 0.16 \pm 0.04 \pm 0.21$
	$\bar{D}^0K^{*0}$	C		$0.20 \pm 0.01 \pm 0.04 \pm 0.01 \pm 0.05$

(i) for $\bar{B} \to DK$, $\bar{B} \to D\pi$, $\bar{B}_s \to D_sK$, and $\bar{B}_s \to D_s\pi$,

$$\left|\frac{T^{\bar{B}\to DK}}{V_{cb}V_{us}^*}\right| = \left|\frac{T^{\bar{B}\to D\pi}}{V_{cb}V_{ud}^*}\right| = \left|\frac{T^{\bar{B}_s\to D_sK}}{V_{cb}V_{us}^*}\right| = \left|\frac{T^{\bar{B}_s\to D_s\pi}}{V_{cb}V_{ud}^*}\right|, \tag{37a}$$

$$\left|\frac{C^{\bar{B}\to DK}}{V_{cb}V_{us}^*}\right| = \left|\frac{C^{\bar{B}\to D\pi}}{V_{cb}V_{ud}^*}\right| = \left|\frac{C^{\bar{B}_s\to DK}}{V_{cb}V_{us}^*}\right|; \tag{37b}$$

(ii) for $\bar{B} \to DK^*$, $\bar{B} \to D\rho$, $\bar{B}_s \to D_sK^*$, and $\bar{B}_s \to D_s\rho$,

$$\left|\frac{T^{\bar{B}\to DK^*}}{V_{cb}V_{us}^*}\right| = \left|\frac{T^{\bar{B}\to D\rho}}{V_{cb}V_{ud}^*}\right| = \left|\frac{T^{\bar{B}_s\to D_sK^*}}{V_{cb}V_{us}^*}\right| = \left|\frac{T^{\bar{B}_s\to D_s\rho}}{V_{cb}V_{ud}^*}\right|, \tag{38a}$$

$$\left|\frac{C^{\bar{B}\to DK^*}}{V_{cb}V_{us}^*}\right| = \left|\frac{C^{\bar{B}\to D\rho}}{V_{cb}V_{ud}^*}\right| = \left|\frac{C^{\bar{B}_s\to DK^*}}{V_{cb}V_{us}^*}\right|; \tag{38b}$$

(iii) for the annihilation type decay modes $\bar{B} \to D_sK^{(*)}$ and $\bar{B}_s \to D\pi(\rho)$,

$$\left|\frac{E^{\bar{B}\to D_sK}}{V_{cb}V_{ud}^*}\right| = \left|\frac{E^{\bar{B}_s^0\to D\pi}}{V_{cb}V_{us}^*}\right|, \tag{39a}$$

$$\left|\frac{E^{\bar{B}\to D_sK^*}}{V_{cb}V_{ud}^*}\right| = \left|\frac{E^{\bar{B}_s^0\to D\rho}}{V_{cb}V_{us}^*}\right|. \tag{39b}$$

To estimate the SU(3) breaking effect, we use the χ^2 fit results and obtain

$$\left|\frac{T^{\bar{B}\to DK}}{V_{cb}V_{us}^*}\right| : \left|\frac{T^{\bar{B}\to D\pi}}{V_{cb}V_{ud}^*}\right| : \left|\frac{T^{\bar{B}_s\to D_sK}}{V_{cb}V_{us}^*}\right| : \left|\frac{T^{\bar{B}_s\to D_s\pi}}{V_{cb}V_{ud}^*}\right| = 1 : 0.83 : 1.10 : 0.90; \tag{40a}$$

$$\left|\frac{C^{\bar{B}\to DK}}{V_{cb}V_{us}^*}\right| : \left|\frac{C^{\bar{B}\to D\pi}}{V_{cb}V_{ud}^*}\right| : \left|\frac{C^{\bar{B}_s\to DK}}{V_{cb}V_{ud}^*}\right| = 1 : 0.85 : 0.91; \tag{40b}$$

$$\left|\frac{T^{\bar{B}\to DK^*}}{V_{cb}V_{us}^*}\right| : \left|\frac{T^{\bar{B}\to D\rho}}{V_{cb}V_{ud}^*}\right| : \left|\frac{T^{\bar{B}_s\to D_sK^*}}{V_{cb}V_{us}^*}\right| : \left|\frac{T^{\bar{B}_s\to D_s\rho}}{V_{cb}V_{ud}^*}\right| = 1 : 0.83 : 1.07 : 0.89; \tag{40c}$$

$$\left|\frac{C^{\bar{B}\to DK^*}}{V_{cb}V_{us}^*}\right| : \left|\frac{C^{\bar{B}\to D\rho}}{V_{cb}V_{ud}^*}\right| : \left|\frac{C^{\bar{B}_s\to DK^*}}{V_{cb}V_{ud}^*}\right| = 1 : 0.79 : 0.84; \tag{40d}$$

$$\left|\frac{E^{\bar{B}\to D_s K}}{V_{cb}V_{ud}^*}\right| : \left|\frac{E^{\bar{B}_s\to D\pi}}{V_{cb}V_{us}^*}\right| = 1:0.81; \tag{40e}$$

$$\left|\frac{E^{\bar{B}\to D_s K^*}}{V_{cb}V_{ud}^*}\right| : \left|\frac{E^{\bar{B}_s^0\to D\rho}}{V_{cb}V_{us}^*}\right| = 1:0.80. \tag{40f}$$

The above results show that the SU(3) symmetry breaking in $\bar{B}\to DM$ is about $10\sim 20\%$ at the amplitude level.

Now, let us look at the SU(3) symmetry breaking in the $B_u^-\to D^0K^-$ and $B_u^-\to D^0\pi^-$, which are related by the so-called U-spin symmetry. For the amplitudes, both T and C topologies contribute to them, and T is proportional to the decay constant of the light meson, while C is proportional to the form factor of B to the light meson. Due to a good approximation $F_0^{B\to K}/F_0^{B\to\pi}\approx f_K/f_\pi$, we then obtain the ratio of the above two processes,

$$\mathcal{R}_1 = \frac{\mathcal{B}(B_u^-\to D^0K^-)/|V_{us}f_K|^2}{\mathcal{B}(B_u^-\to D^0\pi^-)/|V_{ud}f_\pi|^2} = 1.00, \tag{41}$$

which agrees well with the experimental data,

$$\mathcal{R}_1^{\rm exp} = 1.005\pm 0.056. \tag{42}$$

Thus, we conclude that for decay modes dominated by T terms the source of SU(3) symmetry breaking is mainly from the decay constants of light mesons.

In addition, the combination of decay modes $\bar{B}_s^0\to D_s^{*\mp}K^\pm$ and $\bar{B}_s^0\to D_s^{*\mp}\pi^\pm$ [92] is used to test SU(3) symmetry, and the ratios between $\bar{B}_s\to D_s^{(*)\mp}K^\pm$ and $\bar{B}_s\to D_s^\mp\pi^\pm$ are given by

$$\mathcal{R}_2\equiv\frac{\mathcal{B}(\bar{B}_s^0\to D_s^\mp K^\pm)}{\mathcal{B}(\bar{B}_s^0\to D_s^\mp\pi^\pm)},\quad \mathcal{R}_2^*\equiv\frac{\mathcal{B}(\bar{B}_s^0\to D_s^{*\mp}K^\pm)}{\mathcal{B}(\bar{B}_s^0\to D_s^{*\mp}\pi^\pm)}. \tag{43}$$

Under the SU(3) limit, the two ratios are given by [93]

$$\mathcal{R}_2|_{\rm SU(3)} = 0.0864^{+0.0087}_{-0.0072},\quad \mathcal{R}_2^*|_{\rm SU(3)} = 0.099^{+0.030}_{-0.036}. \tag{44}$$

The results we obtained are

$$\mathcal{R}_2|_{\rm FAT} = 0.079^{+0.013}_{-0.005},\qquad \mathcal{R}_2^*|_{\rm FAT} = 0.081^{+0.005}_{-0.003}. \tag{45}$$

Very recently, the LHCb published the latest results on these two ratios [94,95]:

$$\begin{aligned}\mathcal{R}_2|_{\rm Exp} &= 0.0762\pm 0.0015\pm 0.0020,\\ \mathcal{R}_2^*|_{\rm Exp} &= 0.068\pm 0.005^{+0.003}_{-0.002}.\end{aligned} \tag{46}$$

Comparing results of Eqs. (44), (45), and (46), it is obvious that our result for R_2 falls into the range between the SU(3) limit and the experimental data, while for R_2^* both theoretical predictions are larger than the data, which implies that the SU(3) symmetry breaking effect might be more sizable than we expected in these two decays.

C. *CP* asymmetry

Among B_s decays, special attention is paid to the decay modes $\bar{B}_s\to D_s^\pm K^\mp$. As shown in Fig. 3, $B_s^0(\bar{B}_s^0)\to D_s^\pm K^\mp$ decays receive contributions only from T topological amplitudes; in other words, there are no penguin contributions. Note that both B_s^0 and $\bar{B}_s^0$ mesons can decay into the $D_s^+K^-$ final state via CKM matrix elements $V_{ub}V_{cs}$ and $V_{cb}V_{us}$, respectively. They are both of the same order, λ^3, in the Wolfenstein expansion, allowing for large interference effects. Consequently, interference effects between $B_s^0-\bar{B}_s^0$ mixing and decay processes lead to a time-dependent CP asymmetry, which provides sufficient information to determine the weak phase γ in a theoretically clean way. In the following discussion, we set $f=D_s^-K^+$ for simplicity. The time-dependent decay rates of the initially produced flavor eigenstates $|B_s^0(t=0)\rangle$ and $|\bar{B}_s^0(t=0)\rangle$ are given by [96]

$$\begin{aligned}\frac{d\Gamma(B_s^0(t)\to f)}{dt} &= \frac{1}{2}|A_f|^2e^{-\Gamma t}(1+|\lambda_f|^2)\\ &\times\left\{\cosh\left(\frac{\Delta\Gamma t}{2}\right)-D_f\sinh\left(\frac{\Delta\Gamma t}{2}\right)\right.\\ &\left.+C_f\cos(\Delta m_s t)-S_f\sin(\Delta m_s t)\right\},\end{aligned} \tag{47a}$$

$$\begin{aligned}\frac{d\Gamma(\bar{B}_s^0(t)\to f)}{dt} &= \frac{1}{2}|A_f|^2\left(\frac{p}{q}\right)^2e^{-\Gamma t}(1+|\lambda_f|^2)\\ &\times\left\{\cosh\left(\frac{\Delta\Gamma t}{2}\right)-D_f\sinh\left(\frac{\Delta\Gamma t}{2}\right)\right.\\ &\left.-C_f\cos(\Delta m_s t)+S_f\sin(\Delta m_s t)\right\},\end{aligned} \tag{47b}$$

where A_f is the amplitude of $B_s^0\to f$ and the definition of λ_f is

$$\lambda_f = \frac{q}{p}\frac{\bar{A}_f}{A_f} = \frac{q}{p}\frac{A(\bar{B}_s^0\to f)}{A(B_s^0\to f)}. \tag{48}$$

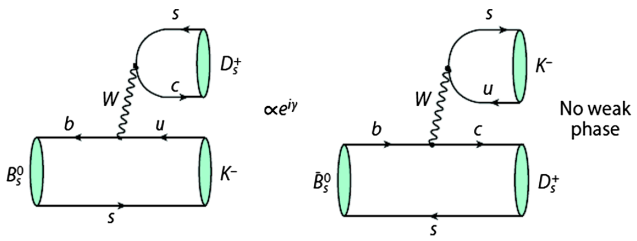

FIG. 3 (color online). Feynman diagrams of $B_s\to D_s^\pm K^\mp$.

The complex coefficients p and q relate the B_s^0 meson mass eigenstates $|B_{H,L}\rangle$ to the flavor eigenstates B_s^0 and $\bar{B}_s^0$,

$$|B_L\rangle = p|B_s^0\rangle + q|\bar{B}_s^0\rangle, \qquad |B_H\rangle = p|B_s^0\rangle - q|\bar{B}_s^0\rangle, \quad (49)$$

and $|p|^2 + |q|^2 = 1$ is satisfied. In the Standard Model, q/p is given by

$$\frac{q}{p} \approx \frac{V_{ts}V_{tb}^*}{V_{ts}^*V_{tb}} \approx e^{-2i\beta_s}. \quad (50)$$

Moreover, Δm_s and $\Delta\Gamma$ denote the mass difference and the total decay width difference of B_H and B_L, respectively. Similar equations can be written for the CP-conjugate decays replacing A_f by $\bar{A}_{\bar{f}} = \langle \bar{f}|\bar{B}_s^0\rangle$, λ_f by $\bar{\lambda}_{\bar{f}} = (p/q)(A_{\bar{f}}/\bar{A}_{\bar{f}})$, $|p/q|^2$ by $|q/p|^2$, C_f by $C_{\bar{f}}$, S_f by $S_{\bar{f}}$, and D_f by $D_{\bar{f}}$. The CP-violation parameters are expressed as [26]

$$C_f = C_{\bar{f}} = \frac{1-|\lambda_f|^2}{1+|\lambda_f|^2}, \quad (51)$$

$$S_f = \frac{2\mathrm{Im}(\lambda_f)}{1+|\lambda_f|^2}, \qquad S_{\bar{f}} = \frac{2\mathrm{Im}(\bar{\lambda}_{\bar{f}})}{1+|\bar{\lambda}_{\bar{f}}|^2}, \quad (52)$$

$$D_f = \frac{2\mathrm{Re}(\lambda_f)}{1+|\lambda_f|^2}, \qquad D_{\bar{f}} = \frac{2\mathrm{Re}(\bar{\lambda}_{\bar{f}})}{1+|\bar{\lambda}_{\bar{f}}|^2}. \quad (53)$$

Note that the equality $C_f = C_{\bar{f}}$ results from $|q/p| = 1$ and $\lambda_f = \bar{\lambda}_{\bar{f}}$. If the above five experimental observables can be measured well and β_s can be measured elsewhere, the CKM angle γ can be extracted. The B_s mixing phase β_s is predicted to be small in the Standard Model [97], and thus we set $\beta_s = -2.5°$ in this work. With the χ^2 fitted result, we then have

$$C_f = C_{\bar{f}} = 0.71 \pm 0.07, \qquad S_f = -S_{\bar{f}} = -0.63 \pm 0.06,$$
$$D_f = D_{\bar{f}} = 0.32 \pm 0.03, \quad (54)$$

where the only uncertainties come from the form factors. In 2011, using a data set corresponding to 1.0 fb^{-1} recorded in pp collisions at $\sqrt{s} = 7$ TeV, the LHCb found the CP-violation observables to be [96]

$$C_f = 1.01 \pm 0.50 \pm 0.23,$$
$$S_f = -1.25 \pm 0.56 \pm 0.24, \qquad S_{\bar{f}} = 0.08 \pm 0.68 \pm 0.28,$$
$$D_f = -1.33 \pm 0.60 \pm 0.26, \qquad D_{\bar{f}} = -0.81 \pm 0.56 \pm 0.26, \quad (55)$$

where the first uncertainties are statistical and the second uncertainties are systematic. Comparing our predictions [Eq. (54)] with the experimental results [Eq. (55)], we find that our results agree with the data within uncertainties. It is should be noted that in our calculation the $|V_{ub}|$ we used is the averaged value of inclusive and exclusive results. However, there is a clear tension between the $|V_{ub}|$ values extracted from the analysis of inclusive and exclusive decays at present, which may lead to large uncertainties in the theoretical calculations.

In addition, the direct CP asymmetries of $B_s^0 \to D_s^{(*)\pm}K^{\mp}$ decays are given by [98]

$$\mathcal{A}_{CP}^{(*)} \equiv \frac{\mathcal{B}(B_s^0 \to D_s^{(*)+}K^-) + \mathcal{B}(\bar{B}_s^0 \to D_s^{(*)+}K^-) - \mathcal{B}(B_s^0 \to D_s^{(*)-}K^+) - \mathcal{B}(\bar{B}_s^0 \to D_s^{(*)-}K^+)}{\mathcal{B}(B_s^0 \to D_s^{(*)+}K^-) + \mathcal{B}(\bar{B}_s^0 \to D_s^{(*)+}K^-) + \mathcal{B}(B_s^0 \to D_s^{(*)-}K^+) + \mathcal{B}(\bar{B}_s^0 \to D_s^{(*)-}K^+)}. \quad (56)$$

In this work, because we set $\chi_c^C = \chi_u^C$ and $\phi_c^C = \phi_u^C$ and ignore the life difference between B_s^0 and $\bar{B}_s^0$, we then get

$$\mathcal{A}_{CP}^{(*)}|_{\mathrm{FAT}} = 0, \quad (57)$$

which agree with the predictions considering the life difference [93]

$$\mathcal{A}_{CP}|_{\mathrm{SU(3)}} = -0.027^{+0.052}_{-0.019}, \qquad \mathcal{A}_{CP}^*|_{\mathrm{SU(3)}} = -0.035^{+0.056}_{-0.024}. \quad (58)$$

So, if in the future, the direct CP asymmetries can be measured at the level of more than 10%, it would be useful to place tighter bounds on the relation between $\chi_c^C e^{i\phi_c^C}$ and $\chi_u^C e^{i\phi_u^C}$.

V. SUMMARY

In the work, we preformed analysis of two-body charmed B decays globally using the factorization-assisted topological-amplitude approach. Since the factorization of the color-favored tree emission diagram has been proven in all orders of the α_s expansion, we use the factorization results of short-distance Wilson coefficients times the decay constant and form factor. For the color-suppressed tree emission and W exchange diagrams, four universal nonperturbative parameters were introduced, namely, χ^C, ϕ^C, χ^E, and ϕ^E, the numerical values of which were fitted from the 31 well-measured branching fractions. With the fitted results, we then predicted the branching fractions of all 120 $B_{u,d,s} \to D^{(*)}P(V)$ decay modes. For the modes induced by the $b \to c$ transition, most results agree with the

experimental data well. The number of free parameters and the χ^2 per degree of freedom are both reduced compared to previous topological diagram analysis. Due to the suppression by CKM element $|V_{ub}|$, the branching fractions of the processes dominated by the $b \to u$ transition are in particular small. Most decays will be measured in the ongoing LHCb experiment and the forthcoming Bell-II experiment. We also found that the SU(3) symmetry breaking is more than 10% and even reaches 31% at the amplitude level. For the decays $\bar{B}_s^0(B_s^0) \to D_s^{\pm}K^{\mp}$, the CP asymmetries predicted agree with the data within uncertainty.

ACKNOWLEDGMENTS

The work is supported by National Natural Science Foundation of China (Grants No. 11175151, No. 11575151, No. 11375208, No. 11521505, No. 11347027, No. 11505083, and No. 11235005) and the Program for New Century Excellent Talents in University (NCET) by Ministry of Education of People's Republic of China (Grant No. NCET-13-0991). Y. Li and C. D. Lu are also supported by the Open Project Program of State Key Laboratory of Theoretical Physics, Institute of Theoretical Physics, Chinese Academy of Sciences, China (Grant No. Y5KF111CJ1).

[1] H.-Y. Cheng and J. G. Smith, Annu. Rev. Nucl. Part. Sci. **59**, 215 (2009).
[2] W. Wang, Int. J. Mod. Phys. A **29**, 1430040 (2014).
[3] A. J. Bevan *et al.* (*BABAR* and Belle Collaborations), Eur. Phys. J. C **74**, 3026 (2014).
[4] R. Aaij *et al.* (LHCb Collaboration), Eur. Phys. J. C **73**, 2373 (2013).
[5] T. Abe *et al.* (Belle II Collaboration), arXiv:1011.0352.
[6] M. J. Dugan and B. Grinstein, Phys. Lett. B **255**, 583 (1991).
[7] M. Wirbel, B. Stech, and M. Bauer, Z. Phys. C **29**, 637 (1985); M. Bauer, B. Stech, and M. Wirbel, Z. Phys. C **34**, 103 (1987).
[8] M. Neubert and B. Stech, Adv. Ser. Dir. High Energy Phys. **15**, 294 (1998).
[9] M. Beneke, G. Buchalla, M. Neubert, and C. T. Sachrajda, Nucl. Phys. **B591**, 313 (2000).
[10] Y. Y. Keum, H. n. Li, and A. I. Sanda, Phys. Lett. B **504**, 6 (2001); C. D. Lu, K. Ukai, and M. Z. Yang, Phys. Rev. D **63**, 074009 (2001); A. Ali, G. Kramer, Y. Li, C. D. Lu, Y. L. Shen, W. Wang, and Y. M. Wang, Phys. Rev. D **76**, 074018 (2007).
[11] C. W. Bauer, D. Pirjol, and I. W. Stewart, Phys. Rev. Lett. **87**, 201806 (2001).
[12] A. J. Buras and L. Silvestrini, Nucl. Phys. **B569**, 3 (2000).
[13] L. L. Chau, H. Y. Cheng, W. K. Sze, H. Yao, and B. Tseng, Phys. Rev. D **43**, 2176 (1991); C. W. Chiang, M. Gronau, J. L. Rosner, and D. A. Suprun, Phys. Rev. D **70**, 034020 (2004); C. W. Chiang and Y. F. Zhou, J. High Energy Phys. 12 (2006) 027.
[14] M. Gronau and D. London, Phys. Lett. B **253**, 483 (1991); M. Gronau and D. Wyler, Phys. Lett. B **265**, 172 (1991); R. Aleksan, I. Dunietz, and B. Kayser, Z. Phys. C **54**, 653 (1992); D. Atwood, I. Dunietz, and A. Soni, Phys. Rev. Lett. **78**, 3257 (1997); D. Atwood, I. Dunietz, and A. Soni, Phys. Rev. D **63**, 036005 (2001); A. Giri, Y. Grossman, A. Soffer, and J. Zupan, Phys. Rev. D **68**, 054018 (2003); C. K. Chua, Phys. Lett. B **633**, 70 (2006).
[15] Y. Amhis *et al.* (Heavy Flavor Averaging Group Collaboration), arXiv:1412.7515.
[16] M. Neubert and A. A. Petrov, Phys. Lett. B **519**, 50 (2001).
[17] C. D. Lü, Phys. Rev. D **68**, 097502 (2003); Y. Y. Keum, T. Kurimoto, H. N. Li, C. D. Lu, and A. I. Sanda, Phys. Rev. D **69**, 094018 (2004).
[18] R. H. Li, C. D. Lu, and H. Zou, Phys. Rev. D **78**, 014018 (2008).
[19] H. Zou, R. H. Li, X. X. Wang, and C. D. Lu, J. Phys. G **37**, 015002 (2010).
[20] C. K. Chua, W. S. Hou, and K. C. Yang, Phys. Rev. D **65**, 096007 (2002); C. K. Chua and W. S. Hou, Phys. Rev. D **77**, 116001 (2008).
[21] C. W. Chiang and E. Senaha, Phys. Rev. D **75**, 074021 (2007).
[22] H. N. Li, C. D. Lü, and F. S. Yu, Phys. Rev. D **86**, 036012 (2012).
[23] H. N. Li, C. D. Lü, Q. Qin, and F. S. Yu, Phys. Rev. D **89**, 054006 (2014).
[24] H. Y. Cheng and C. W. Chiang, Phys. Rev. D **81**, 074021 (2010).
[25] For a review, see G. Buchalla, A. J. Buras, and M. E. Lautenbacher, Rev. Mod. Phys. **68**, 1125 (1996).
[26] K. Olive *et al.* (Particle Data Group), Chin. Phys. C **38**, 090001 (2014).
[27] R. C. Verma, J. Phys. G **39**, 025005 (2012).
[28] H. Y. Cheng, C. K. Chua, and C. W. Hwang, Phys. Rev. D **69**, 074025 (2004).
[29] P. Ball, G. W. Jones, and R. Zwicky, Phys. Rev. D **75** (2007) 054004.
[30] A. Bharucha, D. M. Straub, and R. Zwicky, arXiv: 1503.05534.
[31] M. Jamin and B. O. Lange, Phys. Rev. D **65**, 056005 (2002).
[32] P. Gelhausen, A. Khodjamirian, A. A. Pivovarov, and D. Rosenthal, Phys. Rev. D **88**, 014015 (2013); **89**, 099901 (2014); **91**, 099901 (2015).
[33] W. Lucha, D. Melikhov, and S. Simula, Phys. Lett. B **735**, 12 (2014).
[34] A. A. Penin and M. Steinhauser, Phys. Rev. D **65**, 054006 (2002).
[35] S. Narison, Phys. Lett. B **520**, 115 (2001).

[36] W. Lucha, D. Melikhov, and S. Simula, J. Phys. G **38**, 105002 (2011).
[37] S. Narison, Phys. Lett. B **718**, 1321 (2013).
[38] R. J. Dowdall, C. T. H. Davies, R. R. Horgan, C. J. Monahan, and J. Shigemitsu, Phys. Rev. Lett. **110**, 222003 (2013).
[39] N. Carrasco *et al.*, *Proc. Sci.*, LATTICE2013 (2014) 313.
[40] P. Dimopoulos *et al.* (ETM Collaboration), J. High Energy Phys. 01 (2012) 046.
[41] C. McNeile, C. T. H. Davies, E. Follana, K. Hornbostel, and G. P. Lepage, Phys. Rev. D **85**, 031503 (2012).
[42] A. Bazavov *et al.* (Fermilab Lattice and MILC Collaborations), Phys. Rev. D **85**, 114506 (2012).
[43] H. Na, C. J. Monahan, C. T. H. Davies, R. Horgan, G. P. Lepage, and J. Shigemitsu, Phys. Rev. D **86**, 034506 (2012).
[44] A. Bussone *et al.*, arXiv:1411.5566,
[45] F. Bernardoni *et al.* (ALPHA Collaboration), Phys. Lett. B **735**, 349 (2014).
[46] D. Melikhov and B. Stech, Phys. Rev. D **62**, 014006 (2000).
[47] C. Q. Geng, C. W. Hwang, C. C. Lih, and W. M. Zhang, Phys. Rev. D **64**, 114024 (2001).
[48] C. D. Lu, W. Wang, and Z. T. Wei, Phys. Rev. D **76**, 014013 (2007).
[49] C. Albertus, Phys. Rev. D **89**, 065042 (2014).
[50] H. Y. Cheng and C. K. Chua, Phys. Rev. D **81**, 114006 (2010); **82**, 059904 (2010).
[51] C. H. Chen, Y. L. Shen, and W. Wang, Phys. Lett. B **686**, 118 (2010).
[52] P. Ball and V. M. Braun, Phys. Rev. D **58**, 094016 (1998).
[53] P. Ball, J. High Energy Phys. 09 (1998) 005.
[54] P. Ball and R. Zwicky, J. High Energy Phys. 10 (2001) 019.
[55] P. Ball and R. Zwicky, Phys. Rev. D **71**, 014015 (2005).
[56] P. Ball and R. Zwicky, Phys. Rev. D **71**, 014029 (2005).
[57] P. Ball and G. W. Jones, J. High Energy Phys. 08 (2007) 025.
[58] J. Charles, A. Le Yaouanc, L. Oliver, O. Pene, and J. Raynal, Phys. Rev. D **60**, 014001(1999).
[59] J. L. Rosner, Phys. Rev. D **60**, 074029 (1999).
[60] A. Bharucha, T. Feldmann, and M. Wick, J. High Energy Phys. 09 (2010) 090.
[61] A. Bharucha, J. High Energy Phys. 05 (2012) 092.
[62] A. Khodjamirian, T. Mannel, and N. Offen, Phys. Rev. D **75**, 054013 (2007).
[63] A. Khodjamirian, T. Mannel, N. Offen, and Y.-M. Wang, Phys. Rev. D **83**, 094031 (2011).
[64] Y. M. Wang and Y. L. Shen, Nucl. Phys. **B898**, 563 (2015).
[65] U.-G. Meißer and W. Wang, Phys. Lett. B **730**, 336 (2014).
[66] Y. L. Wu, M. Zhong, and Y. B. Zuo, Int. J. Mod. Phys. A **21**, 6125 (2006).
[67] X. G. Wu and T. Huang, Phys. Rev. D **79**, 034013 (2009).
[68] G. Duplancic, A. Khodjamirian, T. Mannel, B. Melic, and N. Offen, J. High Energy Phys. 04 (2008) 014.
[69] M. A. Ivanov, J. G. Korner, S. G. Kovalenko, P. Santorelli, and G. G. Saidullaeva, Phys. Rev. D **85**, 034004 (2012).
[70] M. Ahmady, R. Campbell, S. Lord, and R. Sandapen, Phys. Rev. D **89**, 074021 (2014).
[71] H. B. Fu, X. G. Wu, and Y. Ma, arXiv:1411.6423.
[72] H. n. Li, Y. L. Shen, and Y. M. Wang, Phys. Rev. D **85**, 074004 (2012).
[73] W. F. Wang and Z. J. Xiao, Phys. Rev. D **86**, 114025 (2012).
[74] W. F. Wang, Y. Y. Fan, M. Liu, and Z. J. Xiao, Phys. Rev. D **87**, 097501 (2013).
[75] Y. Y. Fan, W. F. Wang, S. Cheng, and Z. J. Xiao, Chin. Sci. Bull. **59**, 125 (2014).
[76] Y. Y. Fan, W. F. Wang, and Z. J. Xiao, Phys. Rev. D **89**, 014030 (2014).
[77] T. Kurimoto, H. n. Li, and A. I. Sanda, Phys. Rev. D **65**, 014007 (2001).
[78] T. Kurimoto, H. n. Li, and A. I. Sanda, Phys. Rev. D **67**, 054028 (2003).
[79] C. D. Lu and M. Z. Yang, Eur. Phys. J. C **28**, 515 (2003).
[80] Z. T. Wei and M. Z. Yang, Nucl. Phys. **B642**, 263 (2002).
[81] T. Huang and X. G. Wu, Phys. Rev. D **71**, 034018 (2005).
[82] R. R. Horgan, Z. Liu, S. Meinel, and M. Wingate, Phys. Rev. D **89** 094501 (2014).
[83] E. Dalgic, A. Gray, M. Wingate, C. T. H. Davies, G. P. Lepage, and J. Shigemitsu, Phys. Rev. D **73**, 074502 (2006); **75**, 119906 (2007).
[84] L. Lellouch, arXiv:1104.5484.
[85] S. Aoki *et al.*, Eur. Phys. J. C **74**, 2890 (2014).
[86] F. Ambrosino *et al.*, J. High Energy Phys. 07 (2009) 105.
[87] T. Feldmann, P. Kroll, and B. Stech, Phys. Rev. D **58**, 114006 (1998).
[88] T. Feldmann, P. Kroll, and B. Stech, Phys. Lett. B **449**, 339 (1999).
[89] G. Kramer and C. D. Lu, Int. J. Mod. Phys. A **13**, 3361 (1998).
[90] Y. Fu-Sheng, X. X. Wang, and C. D. Lu, Phys. Rev. D **84**, 074019 (2011).
[91] Z. w. Lin and C. M. Ko, Phys. Rev. C **62**, 034903 (2000).
[92] In fact, the decays $\bar{B}_s^0 \to D_s^{(*)-}\pi^+$ do not exist, and we write them here for symmetrization.
[93] K. De Bruyn, R. Fleischer, R. Knegjens, M. Merk, M. Schiller, and N. Tuning, Nucl. Phys. **B868**, 351 (2013); G. Borissov, R. Fleischer, and M. H. Schune, Annu. Rev. Nucl. Part. Sci. **63**, 205 (2013).
[94] R. Aaij *et al.* (LHCb Collaboration), J. High Energy Phys. 05 (2015) 019.
[95] R. Aaij *et al.* (LHCb Collaboration), J. High Energy Phys. 06 (2015) 130.
[96] LHCb Collaboration, Report No. LHCb-CONF-2012-029; Report No. CERN-LHCb-CONF-2012-029.
[97] A. Lenz and U. Nierste, arXiv:1102.4274.
[98] S. Nandi and U. Nierste, Phys. Rev. D **77**, 054010 (2008).